

SPECIAL ISSUE IN HONOR OF ANDRÉ D. BANDRAUK

Quantum stability of an ion in a Paul trap revisited

A. Hashemloo and C. M. Dion

Department of Physics, Umeå University, SE-901 87 Umeå, Sweden

ARTICLE HISTORY

Compiled September 23, 2018

ABSTRACT

We study the quantum stability of the dynamics of ions in a Paul trap. We revisit the results of Wang *et al.* [Phys. Rev. A **52**, 1419 (1995)], which showed that quantum trajectories did not have the same region of stability as their classical counterpart, contrary to what is obtained from a Floquet analysis of the motion in the periodic trapping field. Using numerical simulations of the full wave-packet dynamics, we confirm that the classical trapping criterion are fully applicable to quantum motion, when considering both the expectation value of the position of the wave packet and its width.

KEYWORDS

Ion trapping; Paul trap; stability

1. Introduction

Paul traps are devices using a radio-frequency, time-dependent electric field to confine charged particles [1–3]. With the right combination of electric potential strength and field frequency, one or many trapped particles will move in closed trajectories inside the trap. Such devices have been used for instance to trap atomic and molecular ions, for studies ranging from mass spectrometry [4], high-precision spectroscopy [5] and ultracold chemistry [6–10] to quantum state manipulation [11, 12] and quantum simulations [13], and recently tests of the time variation of fundamental constants [14].

Of importance is the question of stability. As mentioned above, the motion of a charged particle must be constrained for the particle to be actually trapped. This will depend in particular on the relative electric potentials applied to the electrodes making up the trap and the frequency of the oscillating field. For a classical particle, the motion is given by a Mathieu equation [15], for which stable solutions correspond to cases where the trajectory is bounded. For a quantum particle, the situation is more complicated, but a Floquet analysis [16–19] shows that the average motion of the charged particle follows exactly the classical Mathieu equation, implying that the classical stability criterion also applies in the quantum case. Such a conclusion is also supported by other theoretical derivations [20–22] and numerical simulations of the wave-packet dynamics [23]. While these studies pertain to atomic ions, non-polar molecules have the same centre-of-mass trajectories as atomic ions, and we have also recently shown that the interaction between the trapping field and a dipole moment

doesn't lead to a noticeable modification of the stability criterion [24].

However, a paper by Wang *et al.* [25] purports to show that there are trapping parameters for which a quantum trajectory is stable, while the classical counterpart would not be. Their analysis was based on a study of the convergence of a function series of a dynamical variable related to the wave function of the charged particle. We revisit here this claim by performing a direct simulation of the wave-packet dynamics for the same trapping conditions as considered by Wang *et al.*, as well as by comparing with the corresponding classical trajectories.

This paper is arranged as follows. We start by presenting the trapping model, based on Reference [25], and the corresponding classical stability criterion. The numerical methods corresponding to both quantum and classical simulations are presented in Section 3. This is followed, Section 4, by the results of the various simulations, for stable and unstable trapping parameters. Finally, concluding remarks are given in Section 5.

2. Model for an ion in a Paul trap

2.1. Trapping potential

We consider an ion of charge e and mass m in a two-dimensional Paul trap with the trapping potential [25]

$$V(x, z) = \frac{e}{2r_0^2} (U_0 + V_0 \cos \omega t) (x^2 - z^2), \quad (1)$$

where r_0 is the radius of the trap, U_0 and V_0 the electric potential on the static and radio-frequency electrodes, respectively, with ω the frequency of the time-dependent electric potential. From this point on, we take units such that $e = \hbar = m = r_0 = 1$, and will consider the case $\omega = 5$, the same as for the main results of Reference [25].

2.2. Classical trajectories and stability

The classical equations of motion for the ion are given here by

$$\begin{aligned} \ddot{x} + (U_0 + V_0 \cos \omega t)x &= 0, \\ \ddot{z} - (U_0 + V_0 \cos \omega t)z &= 0. \end{aligned} \quad (2)$$

Using the substitutions

$$a_{x,z} \equiv \pm \frac{4}{\omega^2} U_0, \quad q_{x,z} \equiv \mp \frac{2}{\omega^2} V_0, \quad \tau \equiv \Omega t/2, \quad (3)$$

allows us to rewrite Equations (2) as to Mathieu equations for $\mathbf{r} \equiv (x, z)$,

$$\frac{d^2 \mathbf{r}}{d\tau^2} + (a - 2q \cos 2\tau) \mathbf{r} = 0. \quad (4)$$

Bounded solutions, where \mathbf{r} remains finite, of the Mathieu equation exist for certain regions in the a - q plane [15]. Correspondingly, for certain values of the electric potentials U_0 and V_0 , the ion will remain inside the trap (neglecting possible collisions with

the trap’s electrodes if the amplitude of the motion is too big). This condition is commonly considered the *classical stability region* of an ion trap [1–3], and is the criterion we are using in this paper to label trapping potentials as stable. The boundaries in the a - q plane between stable and unstable regions are given by the Mathieu characteristic values a_r and b_r [15], and the resulting stability diagram is plotted in Figure 1. In this region of the (V_0, U_0) plane, the stability border in x is obtained from a_1 , while the one in z from a_0 . The crossing point is found at $U_0 = 1.48121$, $V_0 = 8.82495$.

3. Numerical methods

We present here a brief description of the simulations of the dynamics of the trapped ion, for both the quantum and classical cases. Further details of the numerical approaches used can be found in Reference [23].

3.1. Quantum mechanical approach

For the quantum wave packet dynamics, we have used the program WAVEPACKET [26], which is based on the split-operator method [27–29], with the wave function expressed on a discrete set of grid points. The Hamiltonian for the motion of the ion is simply

$$\hat{H} = -\frac{1}{2}\nabla_{\mathbf{r}}^2 + V(\mathbf{r}), \quad (5)$$

with $V(\mathbf{r})$ the potential given by Equation (1). While the system considered is two-dimensional, the equations of motion in x and z are separable, and the total wave function is obtained from the combination of two one-dimensional simulations.

To compare the quantum dynamics to the corresponding classical trajectories, we take the initial wave function to be a Gaussian,

$$\psi(x, z; t = 0) = \frac{1}{\sqrt{\pi\sigma_x\sigma_z}} \exp\left[-\frac{(x - x_0)^2}{2\sigma_x^2}\right] \exp\left[-\frac{(z - z_0)^2}{2\sigma_z^2}\right] \quad (6)$$

with $x_0 = z_0 = 1$. We choose the widths $\sigma_x = \sigma_z = 2$, for which the spreading of the wave packet will be reasonable [23]. We use 393216 grid points in the range $[-600, 600]$ along both the x and z axes for the simulations within the stability region, and increase the grid to $[-1600, 1600]$ with 1600000 points for the unstable trajectories. The time step used is $\Delta t = 5 \times 10^{-4}$.

3.2. Classical approach

The expectation values of position $\langle x \rangle$ and $\langle z \rangle$ of the wave packet of the trapped ion can be compared with its classical analogue, given by the Mathieu equations (4). We obtain the classical dynamics by a direct integration of the classical equations of motion (2), using the symplectic Störmer-Verlet integrator [30].

To second order in the time step Δt , the phase-space dynamics for the momentum

\mathbf{p}_n and position \mathbf{r}_n at the n^{th} time step are obtained from [23, 30]

$$\begin{aligned}\mathbf{p}_{n+\frac{1}{2}} &= \mathbf{p}_n - \frac{\Delta t}{2} \mathbf{H}_{\mathbf{r}_n}, \\ \mathbf{r}_{n+1} &= \mathbf{r}_n + \Delta t \frac{\mathbf{p}_{n+\frac{1}{2}}}{m}, \\ \mathbf{p}_{n+1} &= \mathbf{p}_{n+\frac{1}{2}} - \frac{\Delta t}{2} \mathbf{H}_{\mathbf{r}_{n+1}},\end{aligned}\tag{7}$$

where $\mathbf{H}_{\mathbf{r}_n}$ is the vector of partial derivatives of the Hamiltonian $H(\mathbf{p}, \mathbf{q})$ with respect to the components of the position \mathbf{r} ,

$$\begin{aligned}H_{x_n} &= [U_0 + V_0 \cos(\omega t_n)] x_n, \\ H_{z_n} &= -[U_0 + V_0 \cos(\omega t_n)] z_n.\end{aligned}\tag{8}$$

The system of equations (7) is iterated starting from an initial condition equivalent to the quantum simulation (see Section 3.1), namely $\mathbf{r}_0 = (1, 1)$ and $\mathbf{p}_0 = 0$, with a time step $\Delta t = 5 \times 10^{-4}$.

4. Results

Comparing with Figures 1 and 2 of Reference [25], we see that the entire region labelled xz -unstable in Figure 1 is, according to Wang *et al.*, stable for quantum dynamics, since their stability region extends to $U_0 \sim 3.3$. We therefore compare two trapping conditions, one below the crossing between the classically stable and unstable regions (see Section 2.2), the other above.

Taking parameters $\omega = 5$, $U_0 = 1.4811$ and $V_0 = 8.825$, which corresponds to stable trajectories according both to the classical analysis (Figure 1) and that of Reference [25], we find indeed a periodically oscillating, bound trajectory and width of the quantum wave packet, see Figures 2 and 3. There is also a perfect accord (within numerical error) between the classical trajectory and the expectation value of position for the quantum simulation, as calculated by the absolute difference

$$|\langle x \rangle - x_{\text{cl}}|\tag{9}$$

where x_{cl} is the position in the classical trajectory (see Section 3.2), with an equivalent equation in z , as shown in Figures 2(c) and 3(c).

Changing slightly the value of U_0 to 1.4813, the trapping should still be stable quantum mechanically according to Figure 1 of Reference [25], whereas the classical trajectory should be unstable, see Figure 1. The results, presented in Figures 4 and 5, show clearly that, as for all our previous results [23], $\langle x \rangle$ and $\langle z \rangle$ follow exactly the classical motion, and therefore the trajectory is *not* stable. Similarly, the width of the wave packet in both x and z increases continuously, as was seen for a linear Paul trap in Reference [23].

By varying both U_0 and V_0 , we have checked that, in the regions labelled x -stable, z -unstable (or conversely, x -unstable, z -stable) in Figure 1, the dynamical behaviour is as expected, with stability only observed along one of the dimensions. In other words, as far as our simulations show, the quantum wave-packet dynamics follow the stability criteria of the corresponding Mathieu equation for the classical dynamics.

We have also looked at the crossing of the boundary for quantum stability as established by Wang *et al.* [25]. For instance, we have compared the results along z for $U_0 = 0.5$, $V_0 = 2.5$, which should be stable according to Figure 1 of Reference [25], with those for $U_0 = 1$, $V_0 = 2.5$, which lies in the z -unstable region. We have found that both cases lead to unconstrained wave packet dynamics, with no qualitative difference between these two cases. The presence of the boundary presented in Figure 1 of Reference [25] is not observable in our simulations.

5. Conclusion

We have performed quantum simulations of the full dynamics of an ion in a Paul trap, including the time-dependent variation of the trapping potential. We have shown that the centre-of-mass motion of the ion is well reproduced by the classical equations of motion, even outside the so-called stability region, where the trajectories are no longer bound [3].

We have revisited the work of Wang *et al.* [25], and found that even in conditions where they have claimed that there would be a discrepancy between quantum and classical results, we found that the quantum trajectories were equally unstable. This confirms that the classical stability criterion can be applied to quantum motion, both with respect to expectation value of the position and width of the wave packet of the trapped ion.

We conclude that the convergence criterion considered by Wang *et al.* [25] does not inform on the stability of the quantum trajectories, in the usual sense of the capacity of the trap to contain the ion [1–3].

Acknowledgement(s)

The simulations were performed on resources provided by the Swedish National Infrastructure for Computing (SNIC) at the High Performance Computing Center North (HPC2N).

Disclosure statement

No potential conflict of interest was reported by the authors.

Funding

Financial support from Umeå University is gratefully acknowledged.

References

- [1] W. Paul, *Rev. Mod. Phys.* **62** (3), 531–540 (1990).
- [2] P.K. Ghosh, *Ion Traps* (Oxford University Press, Oxford, 1995).
- [3] F.G. Major, V.N. Gheorghe and G. Werth, *Charged Particle Traps: Physics and Techniques of Charged Particle Field Confinement* (Springer, Berlin, 2005).

- [4] R.E. March, *Mass Spectro. Rev.* **28**, 961–989 (2009).
- [5] A. Leanhardt, J. Bohn, H. Loh, P. Maletinsky, E. Meyer, L. Sinclair, R. Stutz and E. Cornell, *J. Mol. Spectrosc.* **270** (1), 1–25 (2011).
- [6] M. Drewsen and A. Brøner, *Phys. Rev. A* **62** (4), 045401 (2000).
- [7] T. Baba and I. Waki, *J. Chem. Phys.* **116** (5), 1858–1861 (2002).
- [8] P. Blythe, B. Roth, U. Fröhlich, H. Wenz and S. Schiller, *Phys. Rev. Lett.* **95** (18), 183002 (2005).
- [9] X. Tong, T. Nagy, J.Y. Reyes, M. Germann, M. Meuwly and S. Willitsch, *Chem. Phys. Lett.* **547**, 1–8 (2012).
- [10] D. Rösch, S. Willitsch, Y.P. Chang and J. Küpper, *J. Chem. Phys.* **140** (12), 124202 (2014).
- [11] D. Leibfried, R. Blatt, C. Monroe and D. Wineland, *Rev. Mod. Phys.* **75** (1), 281–324 (2003).
- [12] D. Leibfried, *New J. Phys.* **14** (2), 023029 (2012).
- [13] C. Schneider, D. Porras and T. Schaetz, *Rep. Prog. Phys.* **75** (2), 024401 (2012).
- [14] N. Huntemann, B. Lipphardt, C. Tamm, V. Gerginov, S. Weyers and E. Peik, *Phys. Rev. Lett.* **113**, 210802 (2014).
- [15] G. Wolf, in *NIST Handbook of Mathematical Functions*, edited by Frank W. J. Oliver, Daniel W. Lozier, Ronald F. Boisvert and Charles W. Clark, Chap. 28 (Cambridge University Press, Cambridge, 2010), pp. 651–681.
- [16] M. Combescure, *Ann. Inst. Henri Poincaré, A* **44** (3), 293–314 (1986).
- [17] L.S. Brown, *Phys. Rev. Lett.* **66** (5), 527–529 (1991).
- [18] R.J. Glauber, in *Laser Manipulation of Atoms and Ions*, edited by E. Arimondo, W. D. Phillips and F. Strumia (North-Holland, Amsterdam, 1992), pp. 643–660.
- [19] R.J. Glauber, in *Quantum Measurements in Optics*, edited by Paolo Tombesi and Daniel F. Walls, *NATO ASI Series B: Physics*, Vol. 282 (Plenum Press, New York, 1992), pp. 3–14.
- [20] F.I. Li, *Phys. Rev. A* **47** (6), 4975–4981 (1993).
- [21] M.M. Nieto and D.R. Truax, *New J. Phys.* **2** (1), 18 (2000).
- [22] W. Hai, S. Huang and K. Gao, *J. Phys. B* **36** (14), 3055 (2003).
- [23] A. Hashemloo, C.M. Dion and G. Rahali, *Int. J. Mod. Phys. C* **27** (2), 1650014 (2016).
- [24] A. Hashemloo and C.M. Dion, *J. Chem. Phys.* **143** (20), 204308 (2015).
- [25] K. Wang, M. Feng and J. Wu, *Phys. Rev. A* **52** (2), 1419–1422 (1995).
- [26] C.M. Dion, A. Hashemloo and G. Rahali, *Comput. Phys. Commun.* **185** (1), 407–414 (2014).
- [27] M.D. Feit, J.A. Fleck, Jr. and A. Steiger, *J. Comput. Phys.* **47** (3), 412–433 (1982).
- [28] M.D. Feit and J.A. Fleck, Jr., *J. Chem. Phys.* **78** (1), 301–308 (1983).
- [29] A.D. Bandrauk and H. Shen, *Chem. Phys. Lett.* **176** (5), 428–432 (1991).
- [30] E. Hairer, C. Lubich and G. Wanner, *Geometric Numerical Integration: Structure-Preserving Algorithms for Ordinary Differential Equations*, 2nd ed. (Springer, Berlin, 2006).

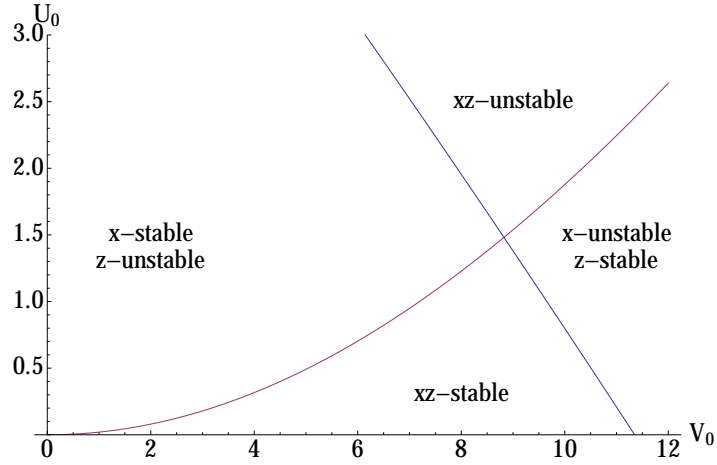


Figure 1. Stability diagram for the Mathieu equation (4) with parameters a and q from Equations (3), calculated for $\omega = 5$ in units where $e = \hbar = m = r_0 = 1$.

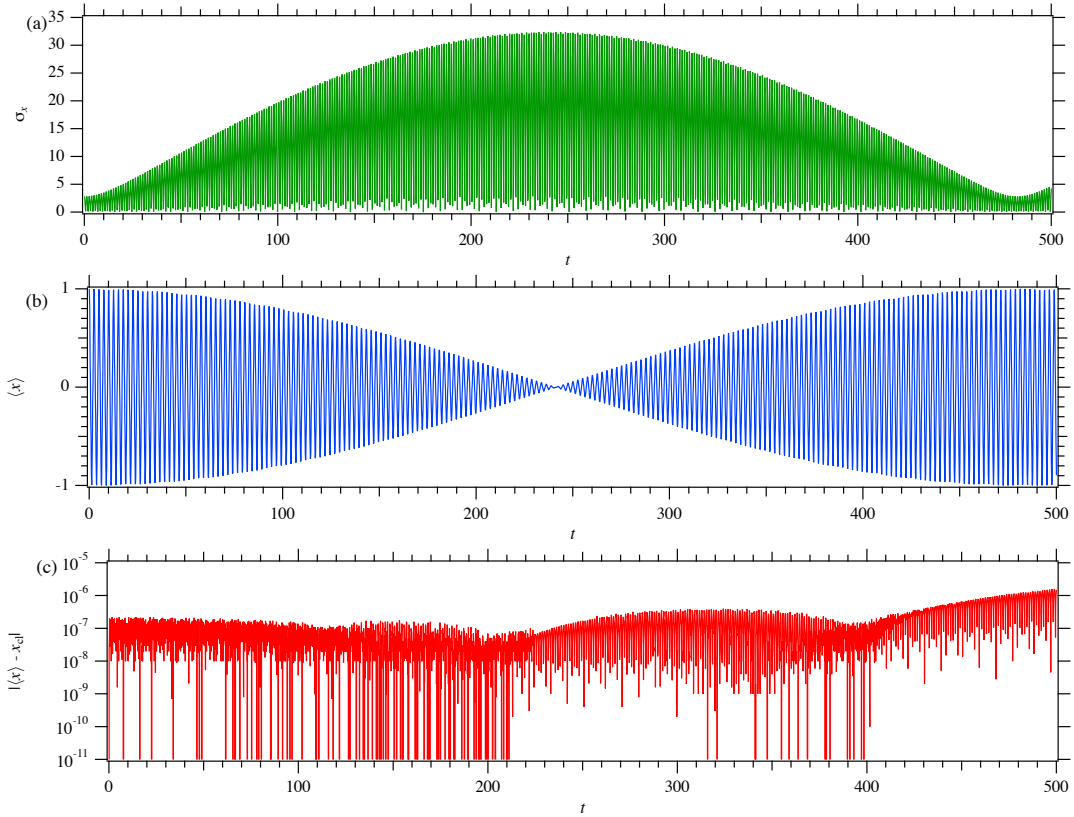


Figure 2. Time evolution of the ion's wave packet along the x axis, for trap parameters $U_0 = 1.4811$ and $V_0 = 8.825$, and $\omega = 5$. (a) Wave-packet width σ_x ; (b) expectation value of the position $\langle x \rangle$; (c) difference between quantum and classical trajectories.

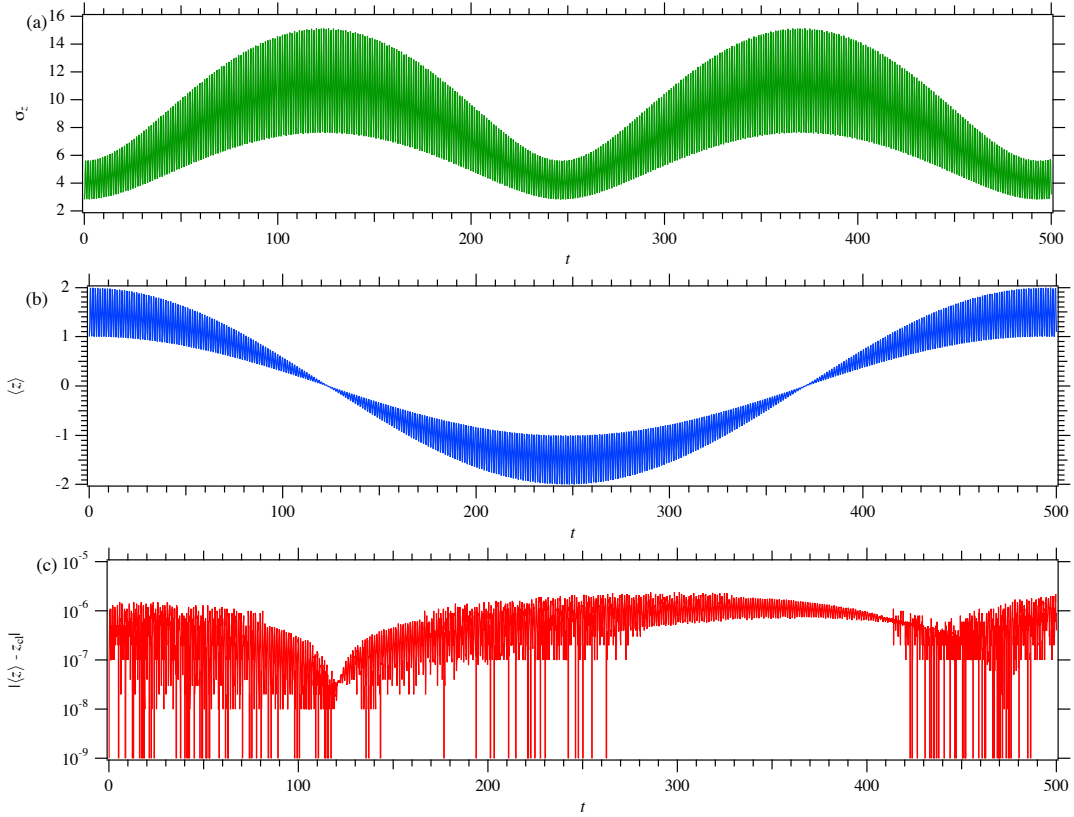


Figure 3. Time evolution of the ion's wave packet along the z axis, for trap parameters $U_0 = 1.4811$ and $V_0 = 8.825$, and $\omega = 5$. (a) Wave-packet width σ_z ; (b) expectation value of the position $\langle z \rangle$; (c) difference between quantum and classical trajectories.

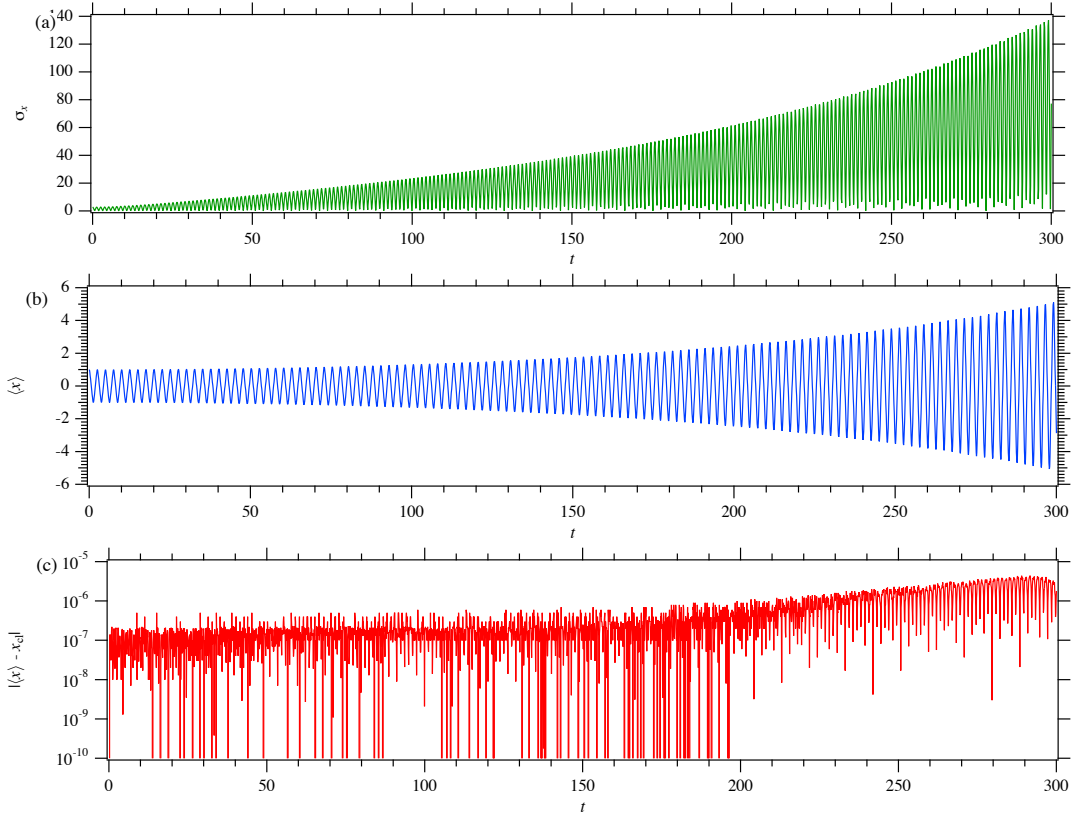


Figure 4. Time evolution of the ion's wave packet along the x axis, for trap parameters $U_0 = 1.4813$ and $V_0 = 8.825$, and $\omega = 5$. (a) Wave-packet width σ_x ; (b) expectation value of the position $\langle x \rangle$; (c) difference between quantum and classical trajectories.

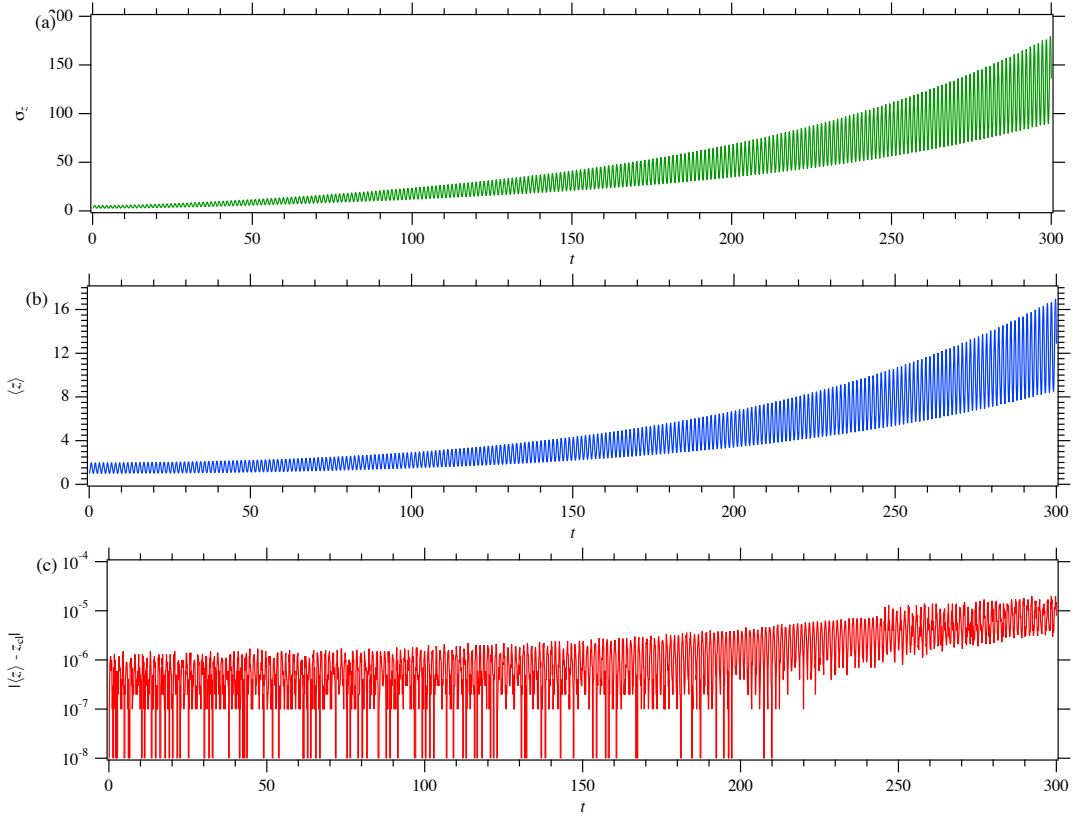


Figure 5. Time evolution of the ion's wave packet along the z axis, for trap parameters $U_0 = 1.4813$ and $V_0 = 8.825$, and $\omega = 5$. (a) Wave-packet width σ_z ; (b) expectation value of the position $\langle z \rangle$; (c) difference between quantum and classical trajectories.